Chemical Science International Journal

29(9): 19-34, 2020; Article no.CSIJ.64469
ISSN: 2456-706X
(Past name: American Chemical Science Journal, Past ISSN: 2249-0205)

Investigation on Chemical, Physical and Biological Assets of a Pioneering biomolecule: (2e)-3-(4-Hydroxy-3-Ethoxyphenyl)-1-(4-Hydroxyphenyl) Prop-2-En-1-One

R. Vasanthi[1], D. Reuben Jonathan[2], S. Sathya[3], B. K. Revathi[4] and G. Usha[1*]

[1]PG and Research Department of Physics, Queen Mary's College, Affiliated to University of Madras, Chennai-04, India.
[2]Department of Chemistry, Madras Christian College, Affiliated to University of Madras, Chennai-59, India.
[3]Department of Physics, Bakthavatchalam College, Affiliated to University of Madras, Chennai - 80, India.
[4]Department of Physics, Madras Christian College, Affiliated to University of Madras, Chennai - 59, India.

Authors' contributions

This work was carried out in collaboration among all authors. Author RV choose the research problem, performed the experiment, data collection and the analysis, wrote the manuscript. Author DRJ managed the chemical synthesis of the compound. Authors SS and BKR contribute to the analyses of the study. Author GU managed the whole manuscript and checked for its correctness and validate the results. All authors read and approved the final manuscript.

Article Information

DOI: 10.9734/CSJI/2020/v29i930203
Editor(s):
(1) Dr. Francisco Marquez-Linares, Universidad Ana G. Méndez, USA.
Reviewers:
(1) Cemal Sandalli, Firtina Research Group, Turkey.
(2) Le Phuong Nguyen, Yonsei University, South Korea.
Complete Peer review History: http://www.sdiarticle4.com/review-history/64469

Original Research Article

Received 25 October 2020
Accepted 30 December 2020
Published 31 December 2020

ABSTRACT

A chalcone derivative, (2E)-3-(4-hydroxy-3-ethoxyphenyl)-1-(4-hydroxyphenyl)prop-2-en-1-one (HEHP), C_{17} H_{16} O_4, has been synthesized from the mixture of 4-hydroxyacetophenone (0.05mol) and 4-hydroxy-3-ethoxybenzaldehyde (0.05mol) and by following Claisen-Schmidt reaction mechanism. Three-dimensional molecular structure, orthorhombic crystal system, and Pbca space

**Corresponding author: E-mail: guqmc@yahoo.com;*

group for the title compound were elucidated via single crystal XRD spectral study. The appearance of the vibration and absorptions for functional groups were identified using the FT-IR spectrum. ^{1}H and ^{13}CNMR spectra were recorded to recognize the number of unique protons and carbon environments and the best estimation of functionality based on shielding/ deshielding effects. The UV-Visible spectral study gives assistance to appreciate the absorbance and transmittance capabilities of the title molecule while Photoluminescence (PL) spectrum of the compound indicates the blue light emission in the visible region. Information regarding the endothermic and exothermic processes correlated with the sample was obtained from TG/DTA thermal analysis and the material was found to be stable up to 216°C. Mechanical properties such as the Hardness (H_V), Meyer's index (n), Newtonian resistance pressure (W), load independent constant (b) and elastic stiffness constant (Cij) were calculated by performing a Vickers hardness test on the compound and they demonstrate excellent mechanical power. The as-synthesized molecule has been screened for its antibacterial, antifungal, and antioxidant activities and observed to exhibit promising activity against various microorganisms

Keywords: Chalcone; ^{1}H, ^{13}C NMR; photoluminescence; TGA/DTA; Vickers microhardness; antioxidant activity.

1. INTRODUCTION

Flavonoids are a group of plant metabolites thought to provide health benefits and antioxidant effects and chalcones are a subclass of Flavonoids. They are α, β-unsaturated ketones consisting of two aromatic rings (ring A and B) having a diverse array of the substituent. Considerable amounts of chalcones present in tomatoes, pears, strawberries, bearberries, and certain wheat products. Chalcones and their derivatives have gained importance because of numerous nutritional and biological benefits. Applications of chalcones are indispensable in medicinal chemistry [1] and they serve as important intermediates for the synthesis of a large number of heterocyclic systems [2]. Chalcones have been extensively studied for their broad spectrum of biological activities [3, 4], including antibacterial [5], antifungal [6], antiparasitic, effect on the functions of the cardiovascular system, antitumor [7], anticancer [7,8],anti-inflammatory [9], anti- leishmanial [10], antitubercular [11], and antioxidant [12] activities. In fact, the pharmacological properties of chalcones are due to the presence of both α, β-unsaturation, and an aromatic ring. The radical quenching properties of the phenolic groups present in many chalcones have raised interest in using the compounds as drugs or food preservatives. A number of chalcones having hydroxy, alkoxy groups in different positions have been observed to possess vasodilatory [13], antifilarial [14], and antimalarial activities [15]. Besides, the lack of advanced data collection facilities and cost-effective instrumentations and software packages, the more thorough investigation regarding the structure-activity relationships, toxicity, and the biological effects could be helpful in designing new compounds for more effective antibacterial, antifungal, antioxidants, and anticancer agents for therapeutic applications.

In view of the wide spectrum of biological demands of the chalcone compounds, the derivative of chalcone (HEHP) has been synthesized by following the acid-catalyzed Claisen-Schmidt reaction and investigated for its optical, thermal, mechanical, and biological properties. In this communication, we report the results of the investigation which have been performed on the title molecule.

2. EXPERIMENTAL

2.1 Synthesis of the Compound (2*E*)-3-(4-Hydroxy-3-Ethoxyphenyl)-1-(4-Hydroxyphenyl) Prop-2-En-1-One (HEHP)

The title compound was synthesized following the published procedure, which uses the acid-catalyzed Claisen-Schmidt reaction [16, 17].The chemicals were purchased from Sigma Aldrich, Chennai, Tamilnadu, India, and used as such without any further purification. Dry HCl gas was made to pass through a well-cooled and stirred solution of 4-hydroxyacetophenone (0.05mol) and 4-hydroxy-3-ethoxybenzaldehyde (0.05mol) in 120 ml of absolute alcohol taken in a 250 Ml round-bottomed flask for a time frame of one hour which aids forming wine red colored solution. In addition of sufficient quantity of ice-cold water yellow coloured precipitate of (2*E*)-3-

(4-hydroxy-3-ethoxyphenyl)-1-(4-hydroxyphenyl) prop-2-en-1-one was formed. The product was filtered, washed with double distilled water, and then allowed to dry. The dried product was re-crystallized from hot ethanol [Yield: 80%; Melting Point: 220°C]. The reaction scheme representing the synthesis procedure is given in Fig. 1

Single crystals of the compound HEHP was grown by slow evaporation solution growth technique. The solution of recrystallized product was prepared at 30°C using absolute ethylmethylketone purchased from Sigma Aldrich, Chennai, Tamilnadu, India as a solvent. The beaker containing the solution was covered and housed in a constant temperature bath (0.1°C) and continuously stirred using Teflon coated immiscible magnetic stirrer purchased from Sigma Scientific products, Chennai, Tamilnadu, India. The temperature was lowered at a rate of 0.5°C/day and after a fortnight, large size crystals were obtained (Fig. 2).

2.2 Details of Characterization Techniques

2.2.1 Spectral characterization

The structural characterization was carried out by X-Ray Diffraction (XRD) while the optical characterization by Proton Nuclear Magnetic Resonance spectroscopy (^{1}HNMR), Carbon-13 Nuclear Magnetic Resonance spectroscopy (^{13}CNMR), Fourier-Transform Infrared spectroscopy (FTIR), Ultraviolet-Visible-Near-IR spectroscopy (UV-VIS-NIR), and Photoluminescence spectroscopy (PL). Mechanical and thermal behaviour of the grown crystal was also investigated.

X-ray diffraction intensity data were collected for the compound using Bruker AXS SMART APEXII single-crystal X-ray diffractometer equipped with graphite monochromated Mo*Kα* (λ=0.7103Å) radiation and CCD detector up to θ_{max}= 28.39°. FTIR spectrum was recorded using Perkin Elmer Spectrometer with KBr pellet technique [18] in the range 4000- 450cm^{-1} from which the functional groups of the compound have been assigned with vibration frequencies. The proton and carbon NMR spectra of the compound were recorded using Bruker Advance III 500 MHz Spectrometer and DMSO-6 as a solvent and the chemical shift for the equivalent protons/carbons with different chemical environments were analyzed. The absorption spectrum of HEHP was recorded in the wavelength range 200-1100 nm using Carry100UV/Vis spectrometer by dissolving the compound in ethanol. The photoluminescence spectrum (PL) of the compound was recorded using the fluorocube lifetime system at SAIF-IITM using the Perkin Elmer - Ls 45 luminescence spectrometer in the range of 200-600 nm. Simultaneous Thermoravimetric analysis (TGA) and Differential thermal analysis (DTA) were carried out for the powdered sample in the temperature range between 38-500°C with a constant heating rate of 10°C/min under a nitrogen atmosphere using a NETZSCH STA 409PC/PG thermal analyzer. The crucible used was made of alumina, which served as a reference for the sample. From the TGA/DTA curve, kinetic as well as thermodynamic parameters were calculated [19, 20]. Mechanical properties of the synthesized compound were studied via the Vickers hardness test at room temperature. The antioxidant activity of the synthesized material has been evaluated using the standard free radical scavenging assay DPPH method [21]. The bacterial/fungal growth inhibition activity was also estimated using the Disk diffusion method on Muller Hinton Agar (MHA) medium [22]/Sabouraud Dextrose Agar (SDA) medium [23].

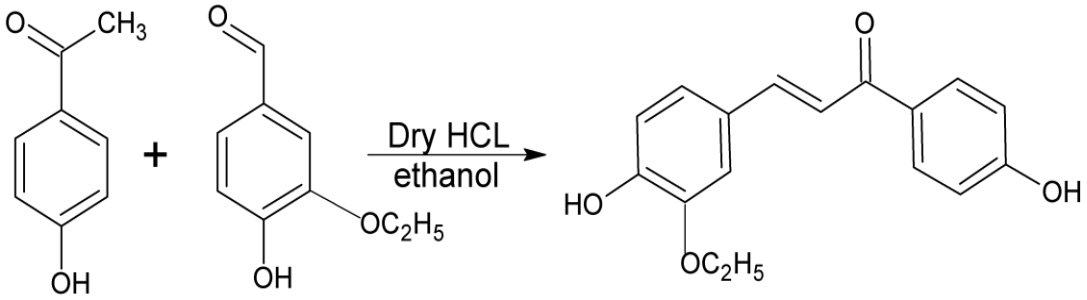

Fig. 1. Reaction scheme of HEHP

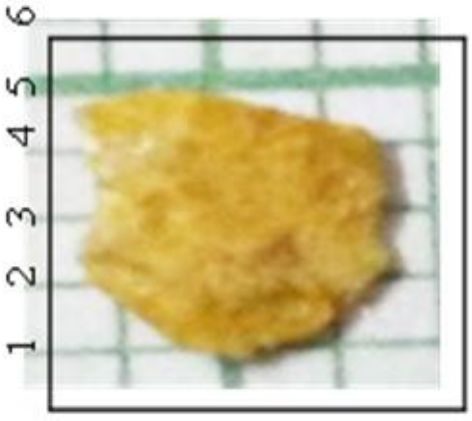

Fig. 2. A grown crystal of HEHP

2.2.2 1,1'- Diphenyl-2-picrylhydrazyl (DPPH) assay

3.7 mL of absolute methanol aliquoted into all test tubes, 100 µL of the sample, and 200 µL of DPPH solution were added to all of the test tubes at room temperature and mixed for 10 s. Thereafter, the test tubes were left at room temperature in the dark. Exactly 30 minutes after the addition of the DPPH solution, the absorbance of the solutions at 517 nm was measured using a UV spectrophotometer /calorimeter for assays. A mixed solution of 100 µL of absolute methanol and 100 µL of Butylated hydroxyl toluene (BHT) was used as the blank. The absorbance at the addition of the analytical sample was expressed as As, the absorbance at the addition of methanol instead of the sample as Ac, and the inhibition ratio (%) was obtained from the following equation:

Inhibition ratio (%) or (%) of antioxidant activity = {(Ac – As)/Ac} ×100

= {(0.96-0.27)/0.96}×100 =71.875%

2.2.3 The *disk diffusion test* on MHA medium/ SDA medium

The title compound was assessed against two Gram-positive bacteria species: *Staphylococcus aureus* and *Bacillus* spp. and three Gram-negative bacteria species: *Salmonella* spp., *E. coli,* and *Pseudomonas* spp / three fungi species: *Candida albicans, Trichoderma viride,* and *Aspergillus niger*. The bacterial/fungus growth inhibition was evaluated for different concentrations (0.5, 0.75 and 1.0mg/mL) of the compound. Disk diffusion method on Muller Hinton agar (MHA) medium/Sabouraud Dextrose agar (SDA) medium employing filter paper disc impregnated with the test compound and wells in dishes were adopted to test the antibacterial/antifungal activity of the title compound. In this procedure, stock culture was kept at 4°C on nutrient agar slant and the active cultures (inoculums) for experiments were prepared by transferring a loop full of stock culture into the test tubes containing nutrient broth, that were incubated for 24 hours at 37°C. Muller Hinton agar (MHA) medium was poured into the Petri plate and allowed to dry for 5h. After it was solidified, the inoculums were spread on the solid plates with a sterile swab moistened with the bacterial/fungal suspension. The disks with 20 µL of a sample at 1000, 750, and 500 µg/mL concentrations were placed over the MHA/SDA plates and incubated at 37°C for 24h. The compound diffuses from the filter paper into the agar. The concentration of the compound will be highest next to the disk and will decrease as the distance from the disk increases. If the compound is effective against bacteria at a certain concentration, no colonies will grow where the concentration in the agar is greater than or equal to the effective concentration. This is the zone of inhibition and the measure of the diameter of zone of inhibition (mm) details the bacterial/fungal growth inhibition capability of the compound against the microorganisms.

3. RESULTS AND DISCUSSION

3.1 Single Crystal X-Ray Diffraction (XRD)

X-ray diffraction intensity data were collected for the title compound HEHP. The compound was crystallized in orthorhombic system having centrosymmetric space group Pbca with unit cell parameters a=16.367,b=10.551,c=16.615 (Å);α= β=γ=90°; V=2869.32(Å^3). The structure was solved by direct methods SHELXS-97 [24] and refined by SHELXL-14 [25] with the full-matrix least-squares procedure. The significant physical and geometrical parameters were tabulated in Table 1. The selected bond lengths, bond angles, torsion angles and geometry of bonded interactions of the compound were given in Tables 2 and 3, respectively. The thermal ellipsoid plot with a numbering scheme for the compound drawn at 30 % probability level [26] and packing of the molecules viewed along the 'b' axis is given in Figs. 3 and 4, respectively.

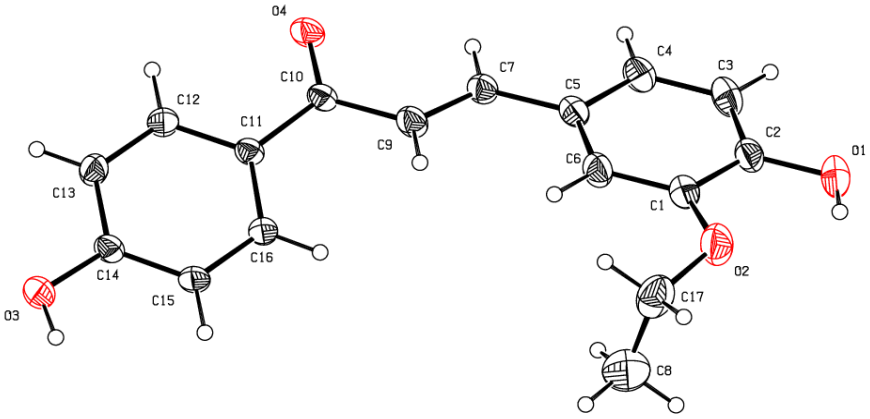

Fig. 3. ORTEP diagram drawn at 30% probability level with numbering scheme

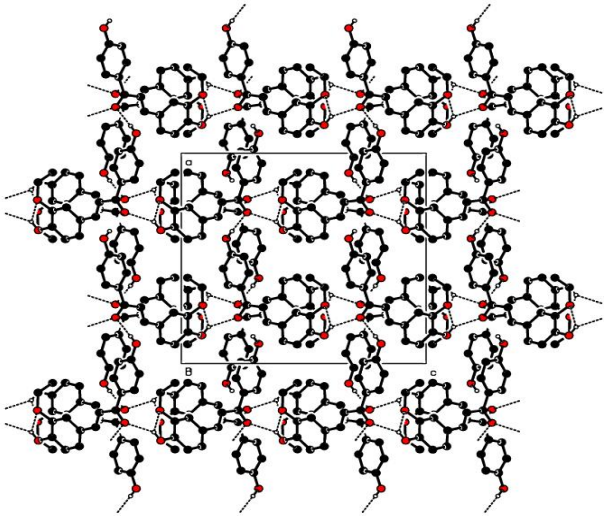

Fig. 4. Packing of the molecules in the unit cell viewed along 'b' axis

Table 1. Physical and geometrical features of the compound HEHP

CCDC No.	**2015948**
Molecular formula	$C_{17}H_{16}O_4$
Chemical diagram	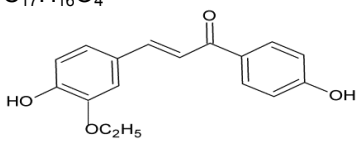
Crystal system	Orthorhombic
space group	Pbca
Goodness-of-fit on F^2	0.724
Final R indices [I>2sigma(I)]	R_1= 0.058 wR_2=0.182
C-C distance of hydroxyphenyl ring	1.376(7) - 1.399(2)Å
C-C distance of ethoxyphenyl ring	1.366(3)-1.408(3)Å
The C-O bond lengths	1.354(2) -1.450(3) Å
The C=O bond length	1.238(2) Å,
Dihedral angle between phenyl rings	21.22 (1)°.

Table 2. Selected bond lengths [Å], bond angles [°] and torsion angles [°] involving non-hydrogen atoms with e.s.d's in the parentheses

Atoms	Bond Distance	Atoms	Bond Angle	Atoms	Torsion angle
C8-C17	1.469(5)	O2-C1-C6	126.71(2)	O2-C1-C2-O1	2.9(3)
C1-O2	1.370(3)	O2-C1-C2	113.72(2)	C6-C1-C2-O1	-179.4(2)
C1-C6	1.377(3)	C6-C1-C2	119.50(2)	O2-C1-C2-C3	-175.8(2)
C1-C2	1.408(3)	O1-C2-C3	119.90(2)	C6-C1-C2-C3	1.9(3)
C2-O1	1.361(2)	O1-C2-C1	120.20(2)	O1-C2-C3-C4	-179.95(1)
C2-C3	1.366(3)	C3-C2-C1	119.88(2)	C1-C2-C3-C4	-1.3(3)
C3-C4	1.387(3)	C2-C3-C4	120.31(2)	C2-C3-C4-C5	-0.6(3)
C4-C5	1.384(3)	C5-C4-C3	120.91(2)	C3-C4-C5-C6	1.8(3)
C5-C6	1.402(3)	C4-C5-C6	118.62(2)	C3-C4-C5-C7	-177.92(1)
C5-C7	1.455(3)	C4-C5-C7	119.44(2)	O2-C1-C6-C5	176.6(2)
C7-C9	1.323(3)	C6-C5-C7	121.93(2)	C2-C1-C6-C5	-0.7(3)
C9-C10	1.467(3)	C1-C6-C5	120.71(1)	C4-C5-C6-C1	-1.1(3)
C10-O4	1.237(2)	C9-C7-C5	127.10(2)	C7-C5-C6-C1	178.6(2)
C10-C11	1.472(2)	C7-C9-C10	123.31(2)	C4-C5-C7-C9	175.3(2)
C11-C16	1.394(2)	O4-C10-C9	121.10(2)	C6-C5-C7-C9	-4.5(3)
C11-C12	1.398(2)	O4-C10-C11	120.50(2)	C5-C7-C9-C10	-177.43(1)
C12-C13	1.378(3)	C9-C10-C11	118.40(2)	C7-C9-C10-O4	-14.2(3)
C13-C14	1.393(3)	C16-C11-C12	117.97(2)	C7-C9-C10-C11	166.32(1)
C14-O3	1.354(2)	C16-C11-C10	122.39(2)	O4-C10-C11-C16	171.05(1)
C14-C15	1.385(3)	C12-C11-C10	119.61(2)	C9-C10-C11-C16	-9.5(3)
C15-C16	1.376(3)	C13-C12-C11	120.93(2)	O4-C10-C11-C12	-10.8(3)
C17-O2	1.450(3)	C12-C13-C14	119.96(2)	C9-C10-C11-C12	168.66(1)
		O3-C14-C15	122.50(2)	C16-C11-C12-C13	0.8(3)
		O3-C14-C13	117.62(2)	C10-C11-C12-C13	-177.40(1)
		C15-C14-C13	119.88(2)	C11-C12-C13-C14	0.1()
		C16-C15-C14	119.71(2)	C12-C13-C14-O3	178.93(19)
		C15-C16-C11	121.54(2)	C12-C13-C14-C15	-1.1(3)
		O2-C17-C8	110.30(3)	O3-C14-C15-C16	-178.90(1)
		C1-O2-C17	118.63(2)	C13-C14-C15-C16	1.1(3)
				C14-C15-C16-C11	-0.1(3)
				C12-C11-C16-C15	-0.8(3)
				C10-C11-C16-C15	177.37(1)
				C6-C1-O2-C17	12.3(4)
				C2-C1-O2-C17	-170.2(2)
				C8-C17-O2-C1	76.2(3)

Table 3. Geometry of the Hydrogen bonds (Å, °)

D-H...A	d(D-H)	d(H...A)	d(D...A)	<(DHA)
O1-H1...O4#1	0.82	2.25	2.958(2)	144
O3-H3A...O4#2	0.82	1.953	2.766(1)	171
O1-H1…O2 (intra)	0.82	2.185	2.646(1)	115

#1 x,-y+5/2, z+1/2 #2 x+1/2, y,-z+1/2

In the compound, atom O1 acts as bifurcated donor forming intra and intermolecular hydrogen bonds with atoms O2 and O4, respectively, and atom O4 behaves as bifurcated acceptor forming intermolecular hydrogen bonds with atoms O3 and O1 of the two neighbouring molecules [Symmetry equivalents: x,-y+5/2, z+1/2; x+1/2, y,-z+1/2]. In the crystal packing, the molecule is linked to four of its adjacent symmetry-related molecules through an O-H…O hydrogen bonds

forming a supramolecular network [Table 3 and Fig. 4].

3.2 Proton and Carbon NMR Spectral Studies

^{1}H NMR (500 MHz, DMSO-d6): *δ*/ppm1.37(t, 3H,-CH_2-CH_3),4.13(q, 2H, -CH_2-CH_3), 9.56(s, 1H, -OH), 10.35(s, 1H,-OH), 6.84(dd, 1H, -C=O-CHα=CH), 7.24(d, 1H, -C=O-CHα=$CH_β$), and7.47-8.06(m, 7H, Ar-H).Besides, the peak at 2.51(s, 1H, -C-C=O) and 3.36(s, 1H, -C-O) are ascribed to the hydrogen α-to carbonyl and α-oxygen, respectively, of the crystal structure. In the present work, the observed chemical shift [Fig. 5a] values of protons of the different chemical environment are in good agreement with the reported values [27-29].

^{13}C NMR (500 MHz, DMSO-d6): *δ*/ppm 15.18 (-CH_2-CH_3), 40.14(O-C), 64.48 (O-CH_2), 162.34 (C=C, unsaturated), 113.20-159.11 (Ar-C), and 187.49 (C=O).The assigned chemical shift [Fig. 5b] values of carbons of the different environment are in good agreement with the reported values [30, 31].

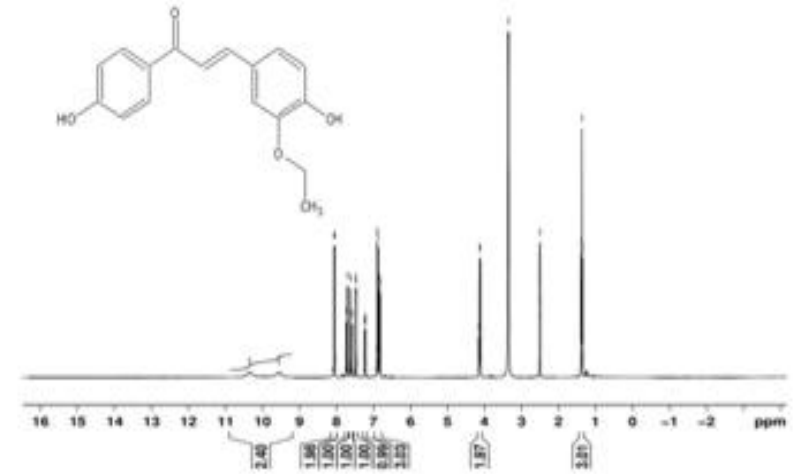

[a]

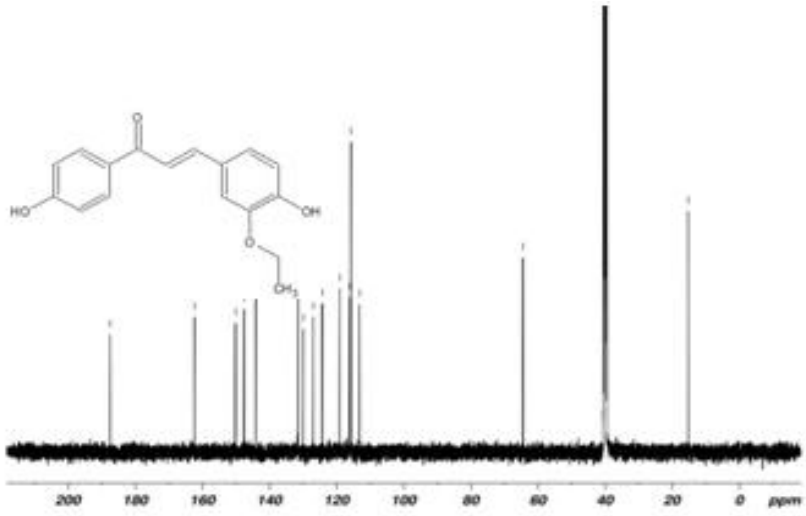

[b]

Fig. 5. [a] Proton and [b] Carbon NMR spectra of HEHP

3.3 FTIR- Spectral Analysis

IR (KBr, cm^{-1}): 3390 and 3162 s (-OH), 2991-2917m (C-H aromatic), 2805-2675 ($-CH_2$), 2456-2077vw ($-CH_3$), 1639s (C=O), 1382 s (C-O), 1268-1271m (C-O-C asymmetric) and 1073-972m (C-O-C symmetric). The absorbance bands [Fig. 6] associated with the functional groups present in HEHP are found to be within the expected range and the assigned wave number values are in good agreement with the reported values [28, 30,32]

3.4 UV-VIS-NIR Spectral Studies

The title compound exhibits prominent excitation peaks at 235 and 361nm (Fig. 7). The existence of two eminent signals is the characteristic feature of flavanoids [33]. The band gap energy was calculated using λ_{max}=361nm in the formula E_g= [12.4237/λc] eV, and is found to be 3.442eV. When the bandgap value is lesser the excitation will be easier and thus longer will be the absorption wavelength. The crystal also shows a good transmittance in the entire visible region which extends even into the near IR region and hence finds applications in optoelectronic devices.

3.5 Photoluminescence Studies

PL spectrum of the title material (Fig. 8) reveals a strong and sharp emission peak at 424nm and a relatively broad peak of medium intensity at 493nm. The first peak is attributed to the transition from excited singlet state to ground state (fluorescence) and the second one to the transition from excited singlet to excited triplet state (intermediate state) and then to ground state (Phosphorescence). The prominent blue emission may be due to the mobility of π-electrons through donor to acceptor groups present in the compound.

3.6 Thermal Analysis

The simultaneously recorded TGA/DTA curve of HEHP is shown in Fig. 9a. The endothermic trend is noted in the DTA curve. A broad exothermic change around 100°C indicates the desorption of water molecules from the compound, whereas the sharp endothermic peak at 221°C specifies the melting point of the compound followed by a broad endothermic peak at 340°C, the decomposition temperature. From the TG thermogram, the large decomposition of mass appears to take place in two steps. A mass change of 33.80% and 19.84% transpire between 216 - 360°C and between 360- 450°C, respectively. From the TG thermogram the upper use temperature observed is 216°C and decomposition of mass extends up to 499°C leaving a residual mass of 44.16%. TGA/DTA thermograms of the grown crystal clearly indicate that the crystal can be utilized for any thermal applications up to 216ºC.

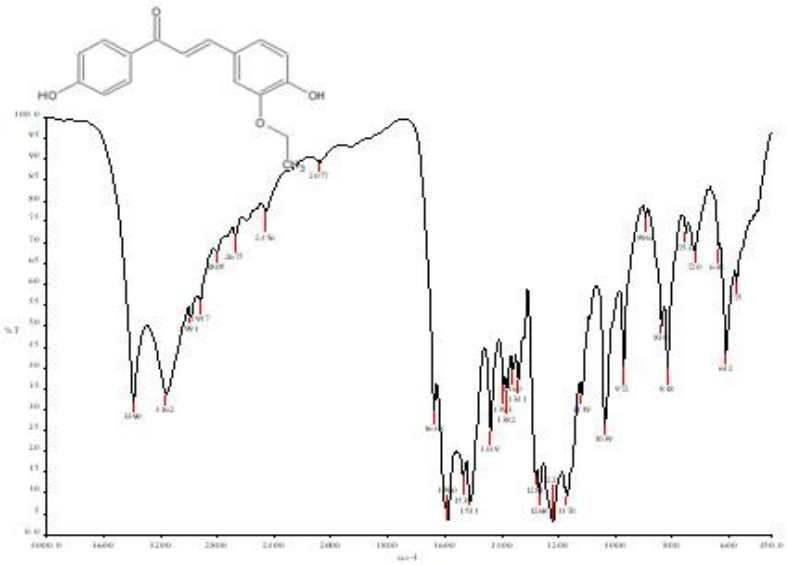

Fig. 6. The recorded FTIR spectrum in the range 4000-400 cm^{-1}, representing the molecular fingerprint of the sample HEHP

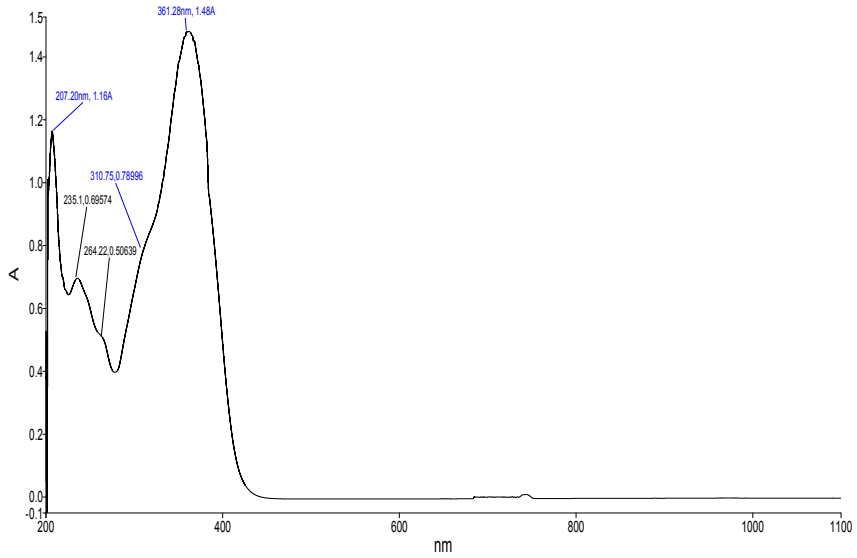

Fig. 7. UV-VIS-NIR spectrum showing absorption bands in the UV region and transmittance in the entire visible region and extended into the near IR region of HEHP

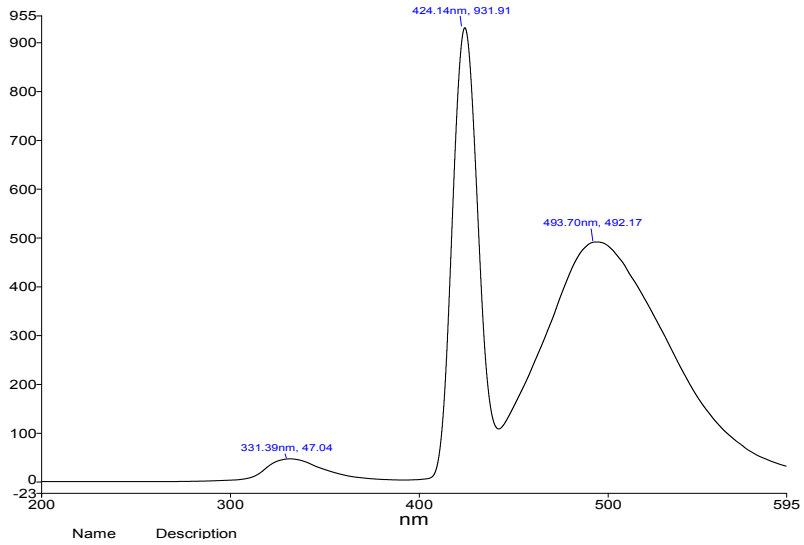

Fig. 8. PL spectrum showing the emission peaks due to fluorescence and Phosphorescence of HEHP

3.6.1 Calculation of kinetic and thermodynamic parameters

TGA of drug materials is probably the largest area of application for thermal analysis and is often used to measure residual solvents and moisture, but can also be used to determine the solubility of drug materials in solvents. These data have been evaluated using the Coats-Redfern relation to obtaining the kinetic parameters as well as thermodynamic properties.

The kinetic parameters like activation energy (E), frequency factor (A) and order of the reaction (n) were determined by Coats and Redfern Relation [34,35]. It also helps to evaluate the thermodynamic properties further. The Coats and Redfern relation is as follows:

$$\log_{10}\left[\left(\frac{\left\{1-(1-\alpha)^{1-n}\right\}}{T^2(1-n)}\right)\right]=\log_{10}\left\{\left(\frac{AR}{\alpha E}\right)\left(1-\frac{2RT}{E}\right)-\left(\frac{E}{2.303RT}\right)\right\}$$

Where, β is the heating rate in K/min, T is the absolute temperature and α is the fraction of original substance decomposed at time t. α.is given by

$$\alpha=\frac{m_o-m_t}{m_o-m_f}$$

here, m_t is the mass at a given time, m_o and m_f is the initial and final masses of the sample respectively, and is calculated from TGA data, and R denotes gas constant. The plots of $Y = -\log_{10}[\{1-(1-\alpha)^{1-n}\}/\{T^2(1-n)\}]$ versus $X=(1/T)10^3\ K^{-1}$, were straight lines for different values of *n,* however, the best linear fit plot gives the correct value of *n*. The activation energy and frequency factor are determined from the slope and intercept of the plot. Using kinetic parameters, the Arrhenius equation can be written as $k = Ae^{-E/RT}$.

For the compound HEHP, the best linear fit was obtained for n = 0.5 (Fig. 9b). The values of activation energy and frequency factor are found to be 84.42 $kJmol^{-1}$ and $2.381x10^{-5}S^{-1}$, respectively. The frequency factor, which can be further used in the calculations of different thermodynamic properties such as entropy ΔS, enthalpy ΔH, Gibbs free energy ΔG and whose values are -329.7,-49.88, and 93.93 (kJ/mol), respectively. They are calculated from the formulae,

$$\Delta S=2.303\times R\times Ah\ K_B\ T_m\ ;\ \Delta H = E - 2\ R\ T;\ \Delta G = \Delta H - T\Delta S$$

where, A is the frequency factor, K_B- Boltzmann constant, h -Planck's constant, R- gas constant, T_m absolute temperature in Kelvin. The Negative value of ΔH reveals that the process is exothermic and that of ΔS shows that the activity is non-spontaneous. Moreover, the positive value of ΔG indicates that the substance is thermodynamically stable [36].

3.7 Vickers Microhardness Test

During the mechanical strength analysis, a diamond indenter is pressed into the surface of the crystal under the influence of a known load (25-100g) and the size of the resulting indentation is measured. The applied load and the corresponding diagonal length of the indentation are listed in Table 4. The hardness number is calculated from the expression, $H_V = [1.854P/d^2]\ Kg/mm^2$, where P is the applied load in gram and d is the diagonal length in millimetre. The graph is plotted between the load and the hardness number for the grown compound (Fig.10a).

A graph is plotted as log d Vs log P (Fig.10b) whose slope is the measure of Meyer's index 'n' or work hardening coefficient. The value of 'n' lies between 1 and 1.6 for hard materials and is more than 1.6 for soft materials [37]. In the present study, 'n' is found to be 2.32 which show that the compound goes with soft materials. Another graph is also drawn between load P and d^2 (Fig.10c), and the value of W (Newtonian resistance pressure) and b (Load independent constant) are determined from the slope and intercept of the plot [38]. The elastic stiffness constant (C_{ij}) [39] for different loads was calculated using Wooster's empirical formula $Cij = (H_V)^{7/4}$, where i, j are normal components of stress (positive for tensile stresses) and the components with $i \neq j$ are the shear components and the calculated values are listed in Table 4.

Table 4. Parameters defining the Mechanical properties of the compound

Load P (g)	d (mm)	H_V (Kg/mm^2)	C_{ij} (Kg/mm^2)	Work hardening coefficient (n)	Newtonian resistance pressure W (g)
25	24.525	72.7	1810.03		
50	34.195	86.55	2455.94	2.318	0.055
00	44.47	97.6	3030.66		

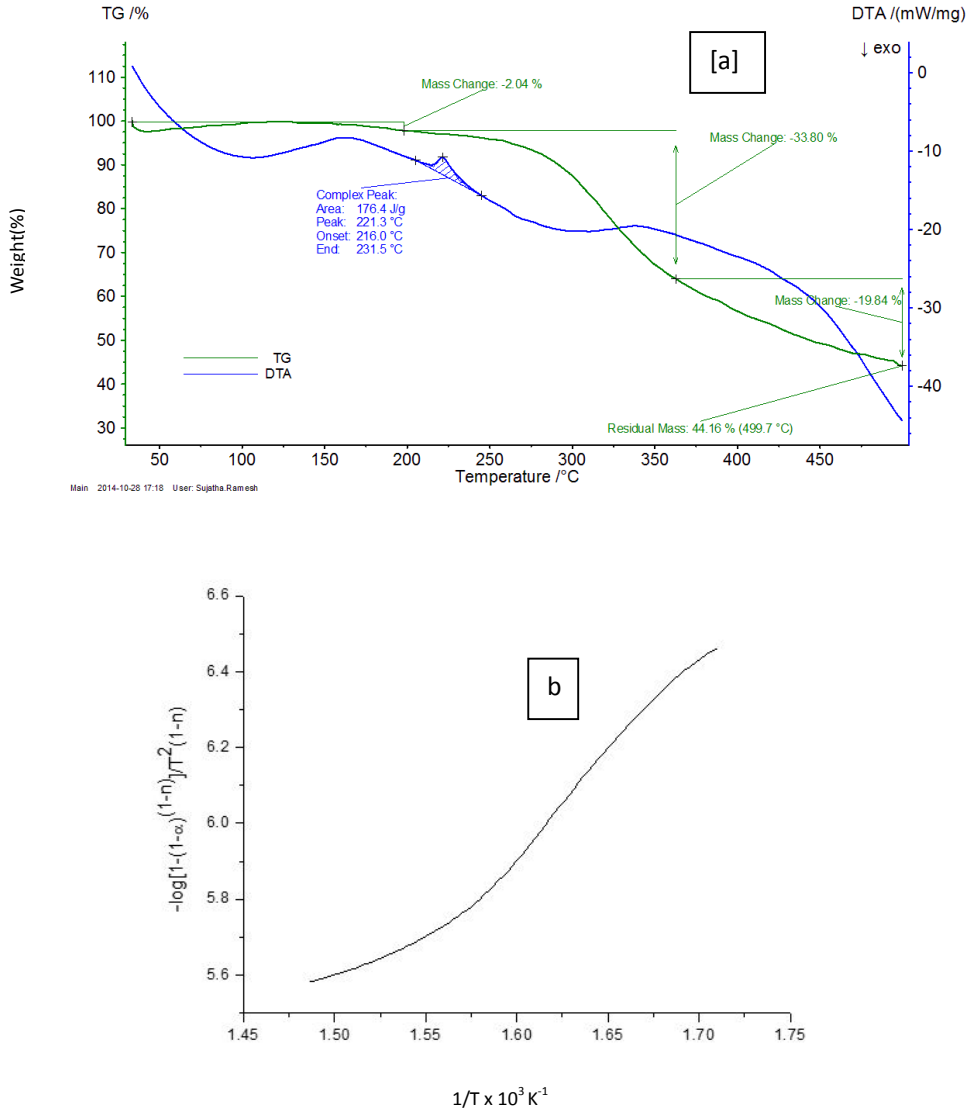

Fig. 9 [a] TG/DTA curves and [b] Plot of coat-redfern relation of HEHP

3.8 Antioxidant Activity Study of the Compound

For the title compound, the percentage of DPPH inhibition which is the measure of the percentage of antioxidant activity was observed to be 71.875%. The *o*- and *p*-substitution by electron-donating groups may increase the antioxidant activities of chalcones [40,41] and the superoxide radical scavenging activity of the chalcones followed the order *o*-methoxychalcone>*m*-methoxy) >*p*-methoxy. The high antioxidant activity of the synthesized compound may be due to the presence of a hydroxyl group that donates an electron to reduce the DPPH radicals. These results offer interesting synthetic possibilities to synthesize more potent antioxidants.

3.9 Antibacterial and Antifungal Activity Studies

Estimated zone of inhibition of the compound against Gram-positive and Gram-negative bacteria/fungi compared with the reference antibiotic drug Ampicillin (1 mg/mL), were listed in Tables 5 & 6. For interpretation of the results the tabulated data were also represented by a bar graph [Fig.11]

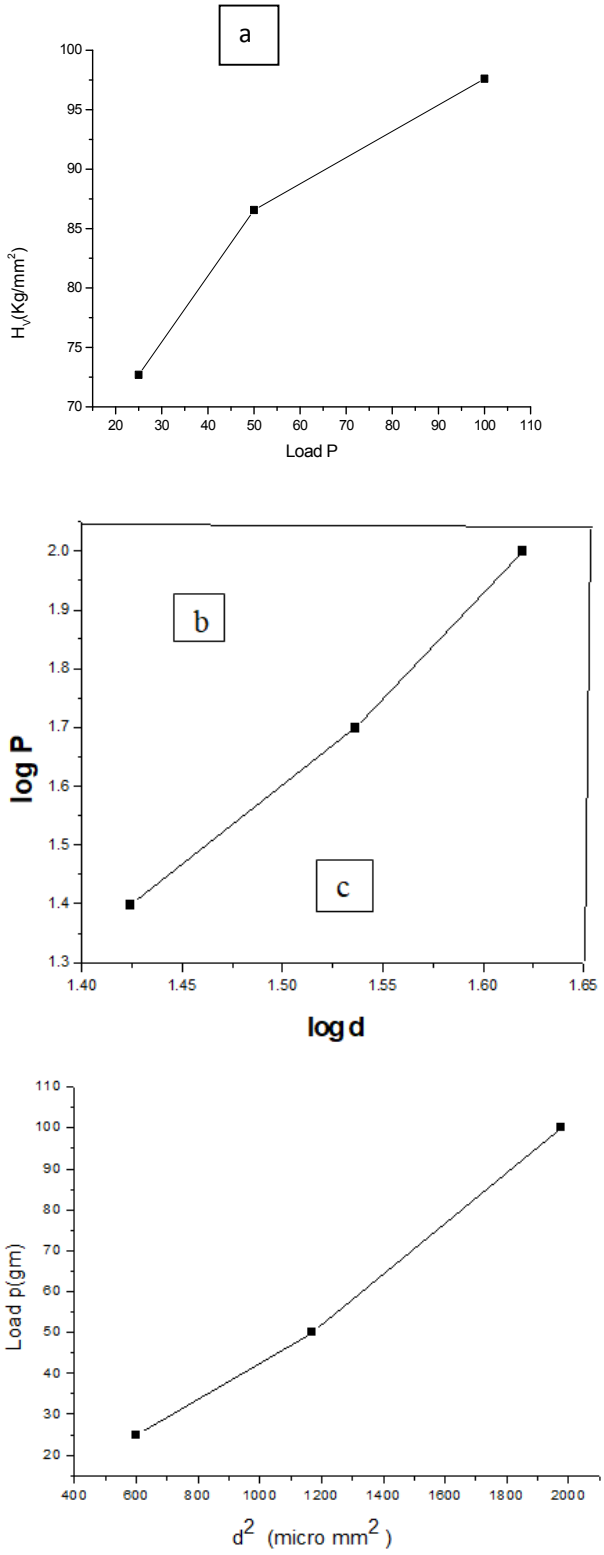

Fig. 10. Plots relating various parameters of HEHP [a] Load P and Hardness number H_v [b] log d and logP [c] d^2 and Load P

Table 5. Antibacterial activity of the compound HEHP

Organisms	Zone of Inhibition (mm) Concentration(mg/mL)			Ampicillin (1mg/mL)
	1.0	0.75	0.5	
Staphylococcus aureus	21	17	17	34
Bacillus spp.	34	21	20	38
E. coli	12	9	7	20
Salmonella spp.	14	12	12	28
Pseudomonas aeroginosa	21	18	16	40

Table 6. Antifungal activity of the compound HEHP

Organisms	Zone of Inhibition (mm) Concentration(mg/mL)			Ampicillin (1mg/mL)
	1.0	0.75	0.5	
Candida albicans	7	6	6	8
Aspergillus niger	14	13	12	15
Trichoderma viride	8	7	6	9

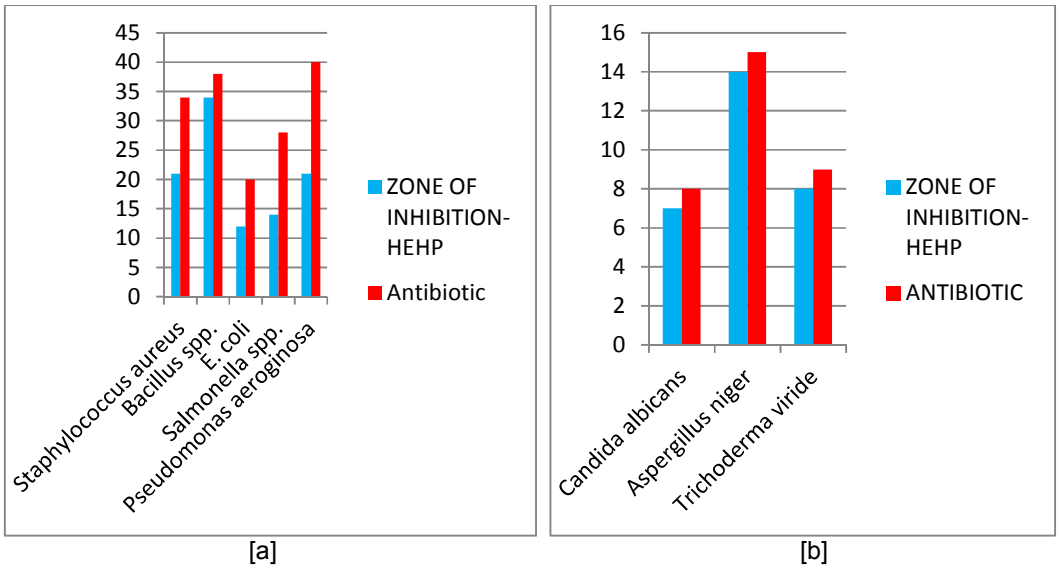

[a] [b]

Fig. 11. Bar Graph: [a] Antibacterial activity of the title compound against various microorganisms and [b] Antifungal activity of the compound against various microorganisms

Chalcone derivative HEHP had shown an excellent bacterial growth inhibition activity against Gram-positive bacterial strains and moderately against Gram-negative bacterial strains. This may be due to the presence of C=O, -OCH_3 and OH groups and the order of bacterial growth inhibition activity for various chalcones had been found X > OH > OCH_3> NO_2 [40,41].

Estimates of the zone of inhibition [Table 6] for the title compound demonstrate the ultimate fungal growth inhibition capability against all fungi. Attaching methoxy group on *p*-position or hydroxyl on any position of the aromatic ring may enhance antifungal activity and the presence of electron-withdrawing groups reduced the activity of chalcones [40,41]. The position of the hydroxyl group in ring A [Fig.3, C11-C16] was found important for chalcone and its derivatives, and the favored location for the hydroxyl group was the *m*-position in ring A. These results reflect that the improvement in antifungal activities of chalcones may be achieved by incorporating hydroxyl and other electron-donating groups at

proper positions in the aromatic rings and avoiding nitro group substitution. In our opinion, it is possible to realize cent percent control over the fungal growth by designing a synthesis procedure incorporating a preferred chemical group at an appropriate position in the aromatic ring of the compound.

4. CONCLUSION

A new chalcone derivative (HEHP) has been synthesized and studied for crystallographic features. The compound was crystallized in the orthorhombic system with the space group Pbca and the crystal packing was stabilized by C-H…O and O-H…O type inter and intramolecular hydrogen bonds. The stretching/bending vibrations of various functional groups of the compound have been assigned with wave numbers via the FTIR spectrum. The chemical shift for the equivalent protons/carbons and the protons/carbons with different chemical environments were analyzed by proton/carbon NMR spectral analysis. The protons/carbons chemical shift values were remaining within the expected range. The absorption and emission capabilities of the grown compound have been analyzed using the UV-Vis-NIR spectrum and the information derived explains its suitability for optoelectronic applications. From the TGA/DTA thermograms, the thermodynamic properties likethe melting point, activation energy, frequency factor, enthalpy, entropy, and Gibb's free energy of the grown compound were calculated. The values of thermodynamic parameters suggest that the chemical process is exothermic, non-spontaneous and the compound is thermodynamically unstable. From the Vickers microhardness test of the compound, the Hardness number (H_V), Meyer's index (n), Newtonian resistance pressure (W), load independent constant (b), and elastic stiffness constant (Cij) were calculated which characterizes its mechanical behavior. Meyer's index ($n > 1.6$) value shows that the crystal fits into soft class material.

The free radical scavenging (antioxidant) activity of the compound was found to be significant (71.875%).The compound has also been evaluated for its antibacterial /antifungal activity and the estimates of the zone of inhibition due to various microorganisms cogitate about excellent to moderate level. It is now possible to produce chalcones at a large scale with the use of genetic modifications; future optimization of chalcones through structural alteration may allow the development of pharmacologically acceptable drugs.

ACKNOWLEDGEMENT

Authors thank SAIF, IIT-Madras, Chennai-36 and DST-FIST, Queen Mary's College (A), Chennai-4 for providing instrumentation facilities.

COMPETING INTERESTS

Authors have declared that no competing interests exist.

REFERENCES

1. Ansari FL, Nazir S, Noureen H, Mirza B, Combinatorial synthesis and antibacterial evaluation of an indexed chalcone library, chem. Biodivers. 2005;2:1656-1664. Available:https://doi.org/10.1002/cbdv.200590135
2. Kachadourian R, Day BJ, Pugazhenti S, Franklin CC, Genoux-Bastide E, Mahaffey G, Gauthier C, Pietro AD, Boumendjel A. A synthetic chalcone as a potent inducer of glutathione biosynthesis. J. Med. Chem. 2012;551:382-1388. Available:https://doi.org/10.1021/jm2016073
3. Nowakowska Z. A review of anti-infective and anti-inflammatory chalcones. Eur. J. Med. Chem. 2007;42:125-137. Available:https://doi.org/10.1016/j.ejmech.2006.09.019
4. Kumar B, Kumari B, Singh N, Ram B, Balram B. Journal of applicable Chemistry. 2014;3(4):1468-1474.
5. Lahtchev KL, Batovska DI, St P Parushev, Ubiyvovk VM, Sibirny AA. Antifungal activity of chalcones: A mechanistic study using various yeast strains. European Journal of Medicinal Chemistry. 2008;43: 2220-2228. Available:https://doi.org/10.1016/j.ejmech.2007.12.027
6. Park EJ, Park HR, Lee JS, Kim J. Licochalcone A: An Inducer of Cell Differentiation and Cytotoxic Agent from Pogostemon cablin1. Planta Med. 1998; 64(5):464-466. Available:https://doi.org/10.1055/s-2006-957485
7. Anto RJ, Sukumarana K, Kuttan G, Rao MNA, Subbaraju V, Kuttan R. Anticancer and antioxidant activity of synthetic

chalcones and related compounds. Cancer Letters. 1995;97:33-37.
Available:https://doi.org/10.1016/0304-3835(95)03945-S

8. Hsieh HK, Tsao LT, Wang JP, Lin CN. Synthesis and anti-inammatory effect of chalcones. J. Pharm. Pharmacol. 2000;52: 163-171.
Available:https://doi.org/10.1211/0022357001773814
9. Nielsen SF, Christensen SB, Cruciani G, Kharazmi A, Liljefors T. Antileishmanial chalcones: Statistical design, synthesis, and three-dimensional quantitative structure-activity relationship analysis. J. Med. Chem. 1998;41(24):4819-4832.
Available:https://doi.org/10.1021/jm980410m
10. Lin YM, Zhou Y, Flavin MT, Zhou LM, Niea W, Chen FC. Chalcones and flavonoids as anti-tuberculosis agents. Bioorg. Med. Chem. 2002;10:2795–2802.
Available:https://doi.org/10.1016/S0968-0896(02)00094-9
11. Ravichandran R, Rajendran M, Devapiriam D. Studies on chalcone derivatives antioxidant and stability constant. Journal of Chemical, Biological and Physical Sciences. 2013;3(4):2446–2458.
12. Siddiqui AA, Rahman MA, Shaharyar M, Mishra R. Synthesis and anticonvulsant activity of some substituted 3, 5-diphenyl-2-pyrazoline-1-carboxamide derivatives. Chemical Science Journal. CSJ. 2010;8:1-10.
13. Awasthi SK, Mishra N, Dixit SK, Sing A. short report: Antifilarial activity of 1,3-diarylpropen-1-One: Effect on glutathione-s -transferase, a phase II detoxification enzyme. Am. J. Trop. Med. Hyg. 2009; 80(5):764–768.
Available:https://doi.org/10.4269/ajtmh.2009.80.764
14. Lim SS, Kim HS, Lee DU. In vitro antimalarial activity of flavonoids and chalcones. Bull. Korean Chem. Soc. 2007;28(12):2495-2497.
15. Awasthi SK, Mishra N, Kumar B, Sharma M, Bhattacharya A, Mishra LC, Bhasin VK. Potent antimalarial activity of newly synthesized substituted chalcone analogs in vitro. Med Chem Res. 2009;18:407–420.
Available:https://doi.org/10.1007/s00044-008-9137-9
16. Chitra M, Jonathan DR, Rajan YC, Duraipandiyan V. A study on the synthesis and antibacterial evaluation of certain copolyesters containing bischalcone moiety in the main chain. Int. J. Chem. Appl. 2013;5:73-81.
17. Sathya S, Jonathan DR, Prathebha K, Jovita J, Usha G. Crystal structure of (2E)-1-(4-hydroxy-3-methoxyphenyl)-3-(4-hydroxyphenyl) prop-2-en-1-one. Acta Cryst. 2014;70:01158–01159.
Available:https://doi.org/10.1107/S1600536814021953
18. Ingebrigtson DN, Smith AL. Anal. Chem. 1954;26(11):1765–1768.
Available:https://doi.org/10.1021/ac60095a023
19. Ramukutty S, Ramachandran E. Thermal kinetics of gel grown etoricoxib hemihydrate drug crystals. International Journal of Biological & Pharmaceutical Research. 2014;5(10):783-785.
20. Priya MK, Revathi BK, Renuka V, Samuel Asirvatham P. Synthesis, structure elucidation, spectroscopic analysis, thermal and NLO properties of a new piperidine derivative – (4-Methylphenyl) (4-methylpiperidin-1-yl) methanone. Optics and Laser Technology. 2019;111:616–622.
Available:https://doi.org/10.1016/j.optlastec.2018.10.033
21. Heatley NG. A method for the assay of penicillin. Biochem. J. 1944;38:61–65. [PMC free article]
[PubMed] [Google Scholar]
22. Valgas C, De Souza SM, Smânia EFA. Screening methods to determine antibacterial activity of natural products. Braz. J. Microbiol. 2007;38:369–380. [Google Scholar]
23. Magaldi S, Mata-Essayag S, Hartung de Capriles C. Well diffusion for antifungal susceptibility testing. Int. J. Infect. Dis. 2004;8:39–45. [PubMed] [Google Scholar]
24. Sheldrick GM. Shelxs-97 and Shelxl-97, software for crystal structure analysis. Siemens Analyical X-ray Instruments Inc., Madison, Wisconsin; 1997.
25. Sheldrick GM. Crystal structure refinement with SHELXL, Acta Cryst. 2015;C7:13–8.
Available:https://doi.org/10.1107/S2053229614024218
26. Farrugia LJ. Win GX suite for small molecule single-crystal crystallography. J. Appl. Cryst. 1999;32:837-838.
Available:https://doi.org/10.1107/S0021889899006020

27. Azimvand J. Synthesis of some new derivatives of 2-methyl-4H-4-chromenone. Journal of Chemical and Pharmaceutical Research. 2012;4(8):3929-3933.
28. Sathya S, Jonathan DR, Prathebha K, Usha G, Jovita J. (E)-3-(4-Hydroxy-3-methoxyphenyl)-1- (4-hydroxyphenyl)prop-2-en-1-one, Acta Cryst. 2014;E70:0593-0594.
Available:https://doi.org/10.1107/S1600536814008757
29. Al-Majedy Y, Kadhum A, Al-Amiery A, Mohamad A. Synthesis and characterization of some new 4-hydroxy-coumarin derivatives, molecules. 2014;19:11791-11799.
Available:https://doi.org/10.3390/molecules190811791
30. Panchal AD, Kunjadia PD, Patel PM. Synthesis and biological evaluation of chalcone derivatives linked triazoles. Int J Pharm Sci Drug Res. 2011;3:331-337.
31. Renuka V, Revathi BK, Jonathan DR, Priya MK, Asirvatham PS. Synthesis, growth and characterization of a new NLO Active Chalcone Derivative - 4-Chloro-N-{3-[(2E)-3-(Methoxyphenyl)Prop-2-Enoyl]Phenyl} Benzamide Monohydrate. J MoSt. 2019;1176:838-846.
Available:https://doi.org/10.1016/j.molstruc.2018.09.021
32. Shettigar V, Patil PS, Naveen S, Dharmaprakash SM, Sridhar MA, Prasad JS. Crystal growth and characterization of new nonlinear optical chalcone derivative: 1-(4-Methoxyphenyl)-3-(3,4-dimethoxyphe-nyl)-2-propen-1-one, Journal of Crystal Growth. 2006;295:44–49.
Available:https://doi.org/10.1016/j.jcrysgro.2006.06.047
33. Pinheiro PF, Justino GC. Structural analysis of flavonoids and related compounds-a review of spectroscopic applications.
ISBN; 2012.
34. Coats AW, Redfern JP. Kinetic parameters from thermogravimetric data, Nature. 1964;201:68–69.
Available:https://doi.org/10.1038/201068a0
35. Mevada KC, Patel VD, Patel KR. FT-IR, XRD and thermal studies of gelgrown barium tartrate crystals, Arch Phy Res. 2012;3:258-263.
36. Chauhan CK, Joseph KC, Parekh BB, Joshi MJ. Growth and characterization of struvite crystals. Indian J Pure & App Phys. 2008;46:507-512.
37. Onitsch EM. Systematic metallographic and mineralogic structures. Mikroskopie. 1950;5(3-4):94-96.
38. Hays C, Kendall EG. An analysis of knoop hardness, metallography. 1973;6(4):273-282.
39. Ramukutty S, Jeyasudha R, Ramachandran E. Mechanical and thermal kinetic parameters of metformin hydrochloride crystals. RRJPPS. 2014; 3(2):36-40.
40. Berar U. Chalcones: Compounds possessing a diversity in applications, Orbital: The Electronic Journal of Chemistry. 2012;4(3):209-221.
41. Rahman MA. Chalcone: A valuable insight into the recent advances and potential pharmacological activities, chem sci. 2011;J(29)1-16.
Available:http://astonjournals.com/csj

Peer-review history:
The peer review history for this paper can be accessed here:
http://www.sdiarticle4.com/review-history/64469